Progressive renal injury from transgenic expression of human carbonic anhydrase IV folding mutants is enhanced by deficiency of p58^{IPK}

Rupak Datta[a], Gul N. Shah[a], Timothy S. Rubbelke[a], Abdul Waheed[a], Michael Rauchman[b], Alan G. Goodman[c], Michael G. Katze[c], and William S. Sly[a,1]

[a]Edward A. Doisy Department of Biochemistry and Molecular Biology and [b]Department of Internal Medicine, Saint Louis University School of Medicine, St. Louis, MO 63104; and [c]Department of Microbiology, University of Washington School of Medicine, Seattle, WA 98195

Contributed by William S. Sly, February 18, 2010 (sent for review January 22, 2010)

Mutations in the human carbonic anhydrase IV (hCAIV) have been associated with retinal degeneration in an autosomal-dominant form of retinitis pigmentosa (RP17). Prior in vitro cell culture studies confirmed that all of the RP17-associated hCAIV mutations cause protein misfolding, leading to endoplasmic reticulum (ER) stress–induced apoptosis in cells expressing the mutant proteins. To evaluate the physiological impacts of these folding mutants in other carbonic anhydrase IV–producing tissues, we generated two transgenic mouse lines expressing R219S or R14W hCAIV under control of the endogenous hCAIV promoter. Expression of either of these mutant proteins in kidneys caused progressive renal injury in male transgenic mice as evidenced by an age-dependent increase in the tubule cell apoptosis starting at approximately 20 weeks of age and vacuolization throughout the renal cortex in older mice. Up-regulation of the ER chaperone, BiP, was observed in the cells of the renal cortex of the male transgenic mice, suggesting ER stress as a causal factor for the renal injury. The renal injury inflicted by expression of the folding mutants was markedly enhanced by haploinsufficiency of the ER cochaperone p58^{IPK}. The transgenic mice expressing the hCAIV folding mutants on a p58^{IPK} heterozygous background showed extensive renal tubular apoptosis by approximately 10 weeks of age in both male and female mice. These data indicate that expression of the RP17-associated folding mutants of hCAIV can adversely affect tissues beyond the retina and their in vivo proteotoxicity is sensitive to modulation of the protein folding environment of the ER.

apoptosis | autosomal dominant | chemical chaperone | endoplasmic reticulum stress | kidney

Carbonic anhydrase IV (CAIV) was the first identified membrane bound isozyme of the 13 member α-carbonic anhydrase (CA) gene family (1). Like all CAs, CAIV catalyzes the reversible hydration of carbon dioxide: $CO_2 + H_2O \leftrightarrow H^+ + HCO_3^-$. Through this reaction it helps regulate pH homeostasis (e.g., in brain, retina) and carbon dioxide and bicarbonate transport (e.g., in kidney) in different parts of the body (2–4). However, recent evidence indicates that CAIV is nonessential in most of those tissues as a result of its functional complementarity with other membrane carbonic anhydrases (CAs; e.g., CAIX, CAXII, and CAXIV) (2, 4). For example, the function of CAIV was found to be important for normal retinal light response only in the absence of CAXIV which is the primary regulator of pH and CO_2 in retina (4). Similarly, absence of CAIV produced no defect in bicarbonate reabsorption in mice kidney unless coupled with the CAXIV deficiency. Also, Innocenti et al. concluded that complementarity with other CAs made CAIV nonessential for regulation of intraocular pressure based on studies of CAIV's sensitivity to inhibition by a series of CA inhibitors (5).

Therefore, it was initially surprising when a signal sequence mutation (R14W) in human CAIV (hCAIV) was discovered to cosegregate with the disease phenotype in a South African family with an autosomal-dominant form of retinitis pigmentosa (RP17) (6). The association of CAIV with RP17 was confirmed by the identification of two other missense mutations (R67H and R219S) in RP17 patients from unrelated families (7, 8). Explaining how, despite being functionally redundant, mutations in hCAIV can lead to a dominant retinal degenerative disease was thus a challenge. To address this issue, we studied transfected cells expressing the disease associated mutant proteins and made the following observations: (*i*) all the RP17-associated hCAIV mutants were impaired in folding and processing in the endoplasmic reticulum (ER), leading to their defective trafficking to the cell surface; (*ii*) accumulation of the mutant proteins in the ER induced the unfolded protein response (UPR) and resulted in ER stress–induced apoptosis; (*iii*) the ER stress also had a dominant-negative effect on other proteins that transit through ER; and (*iv*) the folding defects of the CAIV mutants could be significantly corrected by treating the cells with chemical chaperones. This treatment also rescued the cells from proteotoxicity. Based on these data, we proposed that toxic gain of function involving ER stress-induced apoptosis is the common mechanism for the pathogenesis of RP17 and that this blinding disease is potentially treatable with chemical chaperone therapy (6, 9, 10).

During ER stress, cells initially respond by up-regulating the UPR signal transduction pathways. However, if the stress is severe or prolonged, they usually undergo apoptosis (11). Whether a cell type will adapt or succumb to ER stress depends on the complex interplay among several factors, including the load of misfolded protein, the chaperone environment, and the redox status of the ER. The outcome of ER stress is also influenced by environmental factors (12). Hence, it was of great interest to explore how the folding mutants of hCAIV, which cause retinal degeneration, affect CAIV-expressing cells in other tissues in which the environment would likely be different. Of particular interest are the renal tubular cells in kidney. CAIV is highly expressed in kidney as a GPI-anchored protein in the lumen of proximal tubules, straight tubules, and cortical/medullary collecting ducts (13). To investigate whether expression of the folding mutants of hCAIV causes pathological and/or functional abnormalities in kidney, we generated transgenic mice expressing either R219S or R14W mutant hCAIV under the control of the endogenous human promoter. These two mutations differ in their locations in the primary sequence (R219S mutation affects the mature portion of hCAIV whereas R14W is a signal sequence mutation; Fig. 1*A*). They also differ in their impacts on the enzymatic activity and folding, R14W being a less severe mutation than R219S (6, 10). How these differences, observed in vitro, affect their proteotoxicity in vivo

Author contributions: R.D., A.W., and W.S.S. designed research; R.D., T.S.R., and M.R. performed research; G.N.S., A.G.G., and M.G.K. contributed new reagents/analytic tools; R.D., A.W., M.R., and W.S.S. analyzed data; and R.D. and W.S.S. wrote the paper.

The authors declare no conflict of interest.

[1]To whom correspondence should be addressed. E-mail: slyws@slu.edu.

This article contains supporting information online at www.pnas.org/cgi/content/full/1001905107/DCSupplemental.

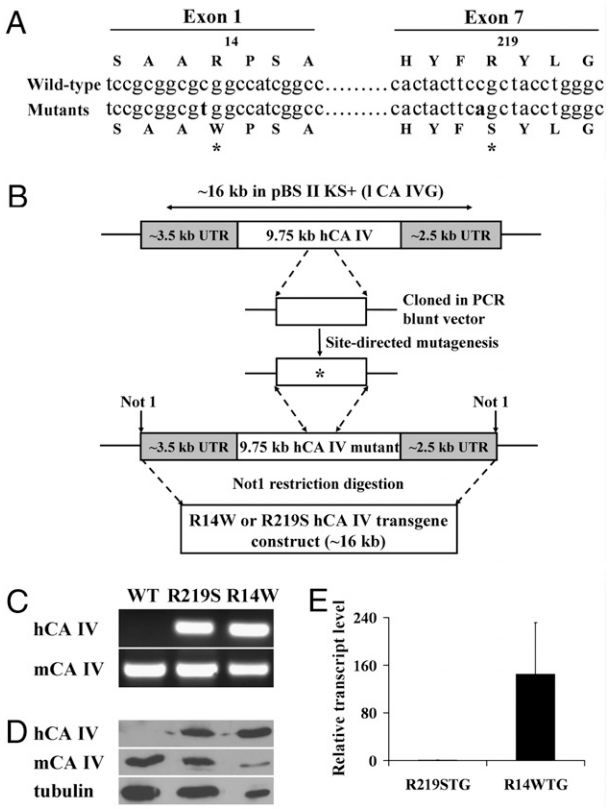

Fig. 1. Construction of transgenic mice and characterization of the transgene expression in the kidney. (*A*) Genomic and protein sequence of hCAIV showing the location of the R219S and the R14W point mutations in the primary sequence. (*B*) Schematic representation of the steps involved in designing of the transgene constructs (see *Materials and Methods* for details). (*C*) RT-PCR analyses of the hCAIV (transgene) and mCAIV (endogenous CAIV) mRNA expression in kidneys from WT, R219STG, or R14WTG mice. (*D*) Western blot analyses of the kidney lysates from WT (100 μg total protein), R219STG (100 μg total protein) or R14WTG (5 μg total protein) mice with antibodies against hCAIV, mCAIV, or tubulin. (*E*) Relative hCAIV transcript levels in kidneys of R219STG and R14WTG mice (three mice in each group) measured by RT-qPCR. Error bars represent SEM.

remains to be tested. Also, whether the proteotoxicity of these folding mutants in vivo can be modulated by changing the chaperone environment of the ER is unknown. Results presented in this article address these unresolved questions, combining genetic and molecular approaches.

Results

Analyses of Transgene Expression in Mouse Kidney. The R219S and R14W hCAIV transgenic mice (R219STG and R14WTG) were generated as described in *Materials and Methods* (Fig. 1*B*). Multiple founders expressing different levels of the transgenes were obtained for both mouse lines. Although analogous results were obtained in different lines of the same genotype, experiments presented in this study were performed on mice from the highest expressing lines. RT-PCR analyses, using primers flanking exons 1a and 3, revealed expression of hCAIV mRNA in kidneys of R219STG and R14WTG mice but not in their WT littermates (Fig. 1*C Top*). As expected, endogenous mouse CAIV (mCAIV) transcripts were detected in all mice (Fig. 1*C Bottom*). The hCAIV protein was also made in the kidneys of both R219STG and R14WTG mice (Fig. 1*D Top*). However, the R219S hCAIV steady-state protein level was much lower than the R14W hCAIV, so much so that the total protein load in the R14WTG lane had to be reduced by 20 fold (compare mCAIV and tubulin levels in Fig. 1*D*) to obtain a uniformly exposed film. As determined by real-time quantitative PCR (RT-qPCR) analyses, the transcript level of R14W hCAIV was more than 100 fold higher than its R219S counterpart (Fig. 1*E*). This low level of R219S hCAIV protein prevented its specific detection by immunohistochemical techniques. However, the R14W hCAIV could easily be detected by immunohistochemistry. The expression of the transgene was restricted to the tubules of the cortex and corticomedullary region of the kidney (Fig. S1).

Changes in Kidney Morphology of the Transgenic Mice with Age. Kidney morphologies of the mice were analyzed by H&E staining and light microscopy (Fig. 2). WT male mice had normal kidney morphology at all ages tested. Kidneys of the young transgenic male mice (<24 weeks) were also normal histologically with no signs of injury. However, the R219STG male mice developed clear vacuoles throughout the renal cortex with aging (>45 weeks), which appeared to coincide with the cells of the proximal tubules. Vacuolations were also observed in the kidneys of older R14WTG male mice, but they were smaller in size and less abundant. The vacuoles appeared empty and none of them contained oil red–positive lipid substances on frozen sections, suggesting that they resulted from tubular cell dropout. Surprisingly, the vacuoles were absent in the kidneys of older transgenic female littermates, implying that renal vacuolization is a male-specific phenotype (Fig. S2 *Top*).

Transgenic Expression of R219S or R14W hCAIV Induces Progressive Renal Apoptosis. Previously we demonstrated that in vitro expression of the folding mutants of hCAIV in HEK293 and COS-7 cells caused abnormal processing in the ER that ultimately led to ER stress–induced apoptosis (6, 10). To examine whether renal tubular cells of the mice carrying the R219S or R14W hCAIV transgene undergo similar cell death, we performed TUNEL staining on the kidney sections of mice at various ages (Fig. 3 *A* and *B*). Our data revealed that the WT mice had minimal evidence of apoptotic cells up to 1 y of age. By contrast, kidneys of both R219STG and R14WTG male mice showed a progressive increase in the number of apoptotic cells beginning at age 20 weeks. Apoptotic nuclei were detected mostly in the renal tubular cells and cells surrounding the tubules in the cortex and corticomedullary junctions of the kidney. Although there was no significant apoptosis in mice analyzed at an age of approximately 10 weeks, at approximately 20 weeks the percentage of TUNEL-positive cells was significantly higher in the male transgenic mice (R219STG, 13.2%; R14WTG, 10.04%) than in their WT littermates (2.97%; $P < 0.001$). The differences in the extent of apoptosis between the WT and the transgenic mice was even larger as the mice grew older (R219STG, 28.49%; R14WTG, 15.11%; WT, 2.58%; $P < 0.001$). It should be noted that the extent

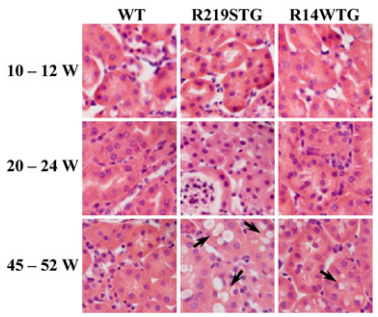

Fig. 2. Histological analyses of kidneys from WT and transgenic mice. Representative H&E-stained kidney sections of male WT, R219STG, or R14WTG mice at various ages in weeks as indicated. Arrows point toward the vacuoles found mostly in the renal cortex.

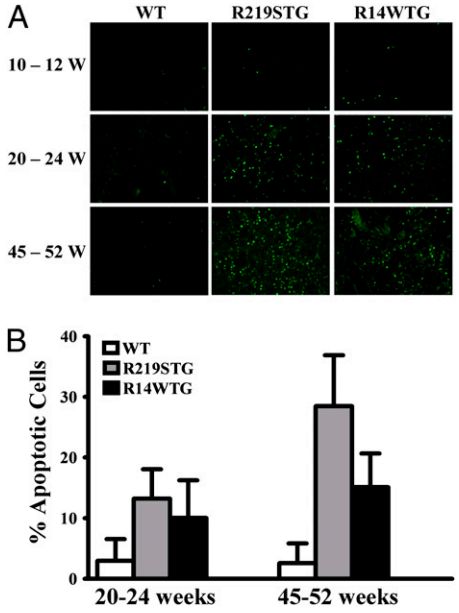

Fig. 3. Evaluation of apoptosis in kidneys of WT and transgenic mice. (*A*) TUNEL staining on tissue sections in kidneys of male WT, R219STG, or R14WTG mice at various ages (in weeks) as indicated. (*B*) Quantitation of apoptotic (i.e., TUNEL-positive) cells expressed as a percentage of total number of DAPI-positive cells in several fields from 4 to 6 mice in each group. Error bars represent SEM.

of apoptosis in old R219STG mice was also significantly greater than in their R14WTG counterparts (28.49% vs. 15.11%; $P < 0.001$). Apoptosis was not detected in any of the female transgenic mice even at 1 y of age (Fig. S2 *Bottom*).

Up-Regulation of ER Stress Marker BiP in Transgenic Mice Kidneys. To examine whether the renal tubular cell death is related to ER stress, we analyzed the transcript levels of the ER chaperone BiP in whole-kidney RNA preparations by RT-qPCR. As shown in Fig. 4*A*, BiP expression was increased by almost threefold ($P < 0.001$) in the kidneys of R219STG mice compared with their WT littermates. The level of BiP in R14WTG mice kidneys was also increased by approximately 1.4 fold, but the difference was not statistically significant ($P = 0.37$). To analyze the level of ER stress in specific areas of kidney, we performed immunohistochemistry on kidney sections with BiP antibody. Immunostaining for BiP protein was markedly increased in the R219STG mice, and the enhanced signal was primarily in the cells of renal cortex. The R14WTG mice also showed evidence of up-regulation in BiP expression, but to a lesser extent (Fig. 4*B*).

Haploinsufficiency of p58^{IPK} Exacerbates the Apoptotic Kidney Damage in Transgenic Mice. As mentioned earlier, renal tubules of R219STG and R14WTG mice showed signs of apoptosis starting at approximately 20 weeks but were completely normal when analyzed at a younger age (approximately 10 weeks). To test whether genetic perturbation of the folding capacity of the ER can enhance sensitivity to the transgene-induced renal damage, we took advantage of the mice deficient for p58^{IPK}, an ER cochaperone of BiP (14, 15). Complete KO of p58^{IPK} (p58$^{IPK-/-}$) in mice has been shown to result in ER stress–induced apoptosis of the pancreatic β-cells, leading to diabetes (14). We observed that the p58^{IPK} KO mice also accumulate autofluorescent materials in their glomeruli, making renal tissues difficult to analyze for the evidence of apoptosis. However, the p58$^{IPK+/-}$ heterozygotes (p58^{IPK}HET) are not diabetic (14) and their kidneys appeared histologically normal. We hypothesized that haploinsufficiency of

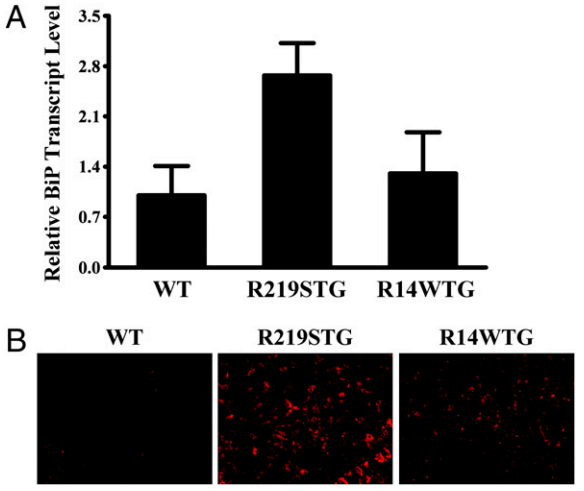

Fig. 4. Induction of the ER stress chaperone BiP in the kidneys of transgenic mice. (*A*) BiP mRNA levels in kidneys of WT, R219STG, or R14WTG mice at approximately 20 weeks of age (three mice in each group) quantified by RT-qPCR. Error bars represent SEM. (*B*) Immunofluorescent detection of BiP expression in representative kidney sections from WT, R219STG, or R14WTG mice at approximately 20 weeks of age.

the cochaperone in the p58^{IPK}HETs would enhance sensitivity to ER stress–induced apoptosis in mice expressing the hCAIV folding mutants. Our results supported this hypothesis. Although p58^{IPK}HETs that did not carry the transgenes showed no evidence of apoptosis at 10 weeks (<1% TUNEL-positive cells), the R219STG/ p58^{IPK}HET or R14WTG/ p58^{IPK}HET mice exhibited a marked increase in the number of apoptotic cells in their renal tubules (31.2% and 29.04%, respectively; $P < 0.0001$) at 10 weeks of age (Fig. 5). Furthermore, the renal damage was no longer restricted to male mice. Kidneys of the p58^{IPK}HET transgenic female mice also showed marked apoptosis at 10 weeks of age. These data indicate that the even 50% reduction of this ER cochaperone can markedly exacerbate the proteotoxicity of the hCAIV folding mutants.

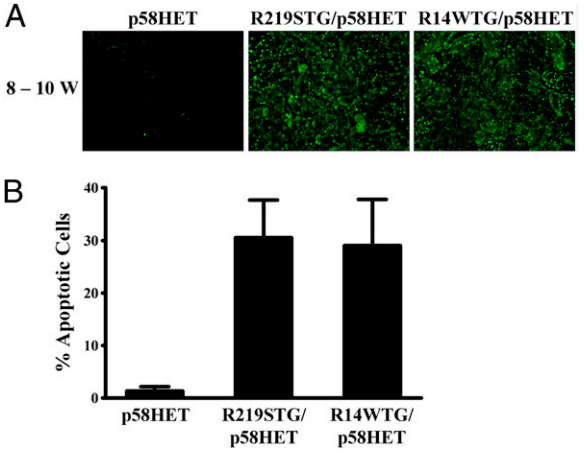

Fig. 5. Haploinsufficiency of p58^{IPK} exacerbates the extent of apoptosis in kidneys of the transgenic mice. (*A*) Representative TUNEL-stained kidney sections of p58^{IPK}HET, R219STG/p58^{IPK}HET, or R14WTG/ p58^{IPK}HET mice at approximately 8–10 weeks age. (*B*) Quantitation of apoptotic (i.e., TUNEL-positive) cells expressed as a percentage of total number of DAPI-positive cells in several fields from three to six mice in each group. Error bars represent SEM.

Discussion

The pathological consequences of the RP17-associated hCAIV mutations extend beyond the retina. We report here that transgenic mice expressing either R219S or R14W hCAIV in their kidneys suffered progressive renal injury. This injury resulted from ER stress–induced apoptosis of the renal tubular cells, which was exacerbated by genetic knockdown of the ER cochaperone $p58^{IPK}$. These results provide clear evidence of in vivo proteotoxicity of these mutant proteins. Additionally, they point toward a critical role of $p58^{IPK}$ in maintaining protein folding homeostasis in renal cells, especially during ER stress.

The R219S and R14W hCAIV were characterized as "folding mutants" based on previous cell culture studies (6, 9, 10). When expressed in Cos-7 or HEK-293 cells, the ER folding/maturation of the R219S hCAIV was drastically impaired such that its cell surface expression was only approximately 10% compared with WT. Its enzymatic activity was also significantly reduced (>90%) (10). In contrast, the R14W was a milder mutation, causing only 30% reduction in enzymatic activity and a similar reduction in the rate of maturation (6). Cells expressing high levels of either of these folding mutants suffered from ER stress–induced apoptosis, which was proposed as the primary cause of retinal degeneration in RP17 patients (6, 10). These findings led to the hypothesis that expression of these mutant proteins would cause similar damage to other tissues in which CAIV is highly expressed. The R219STG and R14WTG mice, designed to mimic the endogenous expression pattern of hCAIV, provided an attractive model to test this hypothesis. As CAIV is abundantly expressed in renal tubular cells, kidney was our focus of attention in the studies reported here.

The kidneys of the R219STG and R14WTG mice appeared normal when they were young (approximately 10 weeks). However, from approximately 20 weeks, their renal tubular cells began to show signs of apoptosis, the extent of which continued to increase as the mice aged. At approximately 1 y, the male transgenic mice had extensive renal injury, evident from the large number of apoptotic cells and vacuolations in the cortex and corticomedullary regions of their kidneys. Although the transgene expression level of the R219S hCAIV was several fold lower than its R14W counterpart, the extent of renal cell death and vacuolation in the R219STG mice was more pronounced than in the R14WTG mice. These data suggest that the in vivo proteotoxicity of the folding mutants is not just an effect of overexpression, but also depends critically on the propensity of the mutant proteins to misfold and the level of ER stress they induce. Indeed, the R219S mutation is conformationally the most destabilizing among all the RP17-associated hCAIV mutations (10). Also, kidneys of R219STG mice expressed a higher level of the ER stress chaperone BiP than those of the R14WTG mice. It is worth noting that these renal abnormalities were seen in only the male mice. None of the female transgenic mice of either genotype showed any signs of morphological abnormality or apoptosis up to 1 y of age. Although the mechanism is still unclear, similar resistance in female mice has been observed in other murine models of ER stress-related proteinopathies (16, 17). One plausible factor for this sex bias might be the testosterone level, which has been shown to modulate various inflammatory and cell death pathways and play a critical role in determining susceptibility to renal ischemic injury (18). Another factor could be sex differences in the level of expression of the transgene. In fact, we observed a threefold higher level of expression of R219S CA IV in kidneys of male transgenic mice compared with their female littermates.

ER stress plays a determining role in development of many renal pathophysiologies involving glomerular or tubular injuries (19, 20). In most of these diseases, ER stress was induced by environmental insults like ischemia reperfusion (21), glucose imbalance (22), heavy metal toxicity (23), or protein overload (24). However, there are some examples in which kidney injuries were caused by proteotoxicity resulting from inherited missense mutations in proteins expressed in the kidney, as reported here. The most common example is congenital nephrotic syndrome of the Finnish type, in which several structural mutations were identified in the podocyte membrane protein nephrin (25). In another recent study, Zivná et al. identified mutations in the signal sequence encoding region of the renin gene in patients with an autosomal-dominant syndrome characterized by anemia, hypouricosuric hyperuricemia, and progressive kidney injury (26). As in our model of proteotoxic renal injury, their study suggested that chronic ER stress resulting from impaired processing of the mutant preprorenin in the ER is the molecular basis of nephron dropout and progressive renal failure seen in their patients (26).

The progressive nature of the renal injury in the R219STG and R14WTG mice reported here is not uncommon among degenerative protein-folding diseases (27, 28). The mechanism might be an age-dependent decline in the UPR-mediated cellular adaptive capacity during ER stress, as has been observed in several organisms including mice, rats, and *Caenorhabditis elegans* (29, 30). If an age-related reduction in adaptive capacity to ER stress is at play, we reasoned we might exaggerate this effect by crossing the mutant transgenes onto a genetic background with a deficiency in an ER chaperone or some component of the UPR. To create this scenario, we crossed the transgenic mice onto a background deficient for $p58^{IPK}$, an ER cochaperone of BiP. We found that haploinsufficiency of $p58^{IPK}$ greatly exacerbated the renal phenotype. The mutant transgenes and $p58^{IPK}$ haploinsufficiency, when combined, induced extensive renal tubular cell death by age 10 weeks in both R219STG/p58HET and R14WTG/$p58^{IPK}$HET mice. Neither the expression of the transgenes nor the $p58^{IPK}$ haploinsufficiency alone had this effect. Furthermore, the proteotoxicities of the mutant transgenes on the $p58^{IPK}$HET background affected female as well as male mice. Thus, reducing the adapting capacity to ER stress makes both male and female mice susceptible to the adverse effects of these folding mutant proteins at an early age. These data are reminiscent of those of Oyadomari et al., who found that deficiency of $p58^{IPK}$ accelerated the development of diabetes in the "Akita mouse" in which diabetes results from a conformational mutation in the insulin 2 gene (31). It will be interesting to study how $p58^{IPK}$ haploinsufficiency affects the retinal injury induced by expression of the hCA IV folding mutants in the retinal choriocapillaries.

The fact that the proteotoxicities of these mutant transgenes are sensitive to alterations in the protein folding environment of the ER gives us the hope that this property can also be used toward developing a therapy. In prior experiments, we provided the proof of concept that chemical chaperones can enhance the adaptive capacity of the transfected mammalian cells and thereby protect them from ER stress–induced apoptosis caused by expression of these folding mutants (9, 10). The transgenic mice expressing these mutant proteins in their kidney provide an attractive model to test the efficacies of the chemical chaperones in vivo. Our hope would be that the chemical chaperones would partially or fully protect the treated mice from the renal pathologies induced by these folding mutations. Such a result could have an impact on patients with known kidney diseases that have a similar mechanism (25, 26).

Materials and Methods

Construction of Mouse Models. For generation of the transgenic mice, R219S or R14W hCAIV transgene constructs were produced from the 16 kb full-length genomic clone of human CAIV (λCAIVG) (32). As described in Fig. 1*B*, a smaller fragment (<5 kb) encompassing the site of the desired point mutation was excised from λCAIVG by using appropriate restriction enzymes (Sph1 double digestion and HindIII/MluI digestion for the R219S and R14W mutations, respectively) and subcloned into PCR blunt vector. The resulting construct served as a template to introduce the R219S and R14W mutations in exons 1 and 7, respectively (Fig. 1*A*) by using QuikChange II site-directed mutagenesis kit (Stratagene) and appropriate primer sets. The mutant fragments were then excised from the PCR blunt vector and swapped with the corresponding WT fragment in λCAIVG. Mutant λCAIVG with inserts in correct orientation were verified by sequencing. All of the exons and intron–exon junctions were

thoroughly sequenced to confirm the absence of any undesired mutations. The transgenes were excised by Not1 restriction digestion and fragments of approximately 16 kb were gel-purified using QiaexII gel extraction kit. R219STG or R14WTG mice were generated by injecting the transgene constructs into the pronuclei of fertilized eggs of C57BL/6 × CBA hybrid mice (Washington University Mouse Genetics Core Facility, St. Louis, MO). Multiple founders were obtained for each of the lines, which were then bred to C57BL/6 background. All transgenic mice were indistinguishable from their WT littermates, were fertile, and produced offspring in expected Mendelian frequencies. Construction of the $p58^{IPK}$ KO mice was described earlier (14). To generate R14WTG or R219STG mice on a $p58^{IPK}$-deficient background, the transgenic mice (either R219STG or R14WTG) were first crossed with $p58^{IPK}$ KO mice to produce $TG^{+}/p58^{IPK}$HET progeny. Successive intercrosses between $TG^{+}/p58^{IPK}$ HET and $p58^{IPK}$ KO mice generated offspring of the following genotypes: $TG^{+}/p58^{IPK}$HET, $TG^{-}/p58^{IPK}$HET, $TG^{+}/p58^{IPK}$KO, and $TG^{-}/p58^{IPK}$KO. Genotypings were performed with genomic DNA extracted from mice tails by using a genomic DNA extraction kit (Sigma-Aldrich). The hCAIV transgene status was identified by the presence of a 529-bp PCR product amplified using the following primers: 5′-AAATTGCGGTGCTGGCCTTTCTGGTGGAGG-3′ (exon 4, forward) and 5′-TCCAACAGGCTGCTCTCTGCCATCGTAGTG-3′ (exon 6, reverse). The $p58^{IPK}$ genotyping was performed as described earlier (14). All animal procedures were performed according to the guidelines of the Saint Louis University Institutional Animal Care and Use Committee.

Western Blotting. Kidneys dissected after PBS perfusion were lysed in cold PBS solution, pH 7.5, and the protease inhibitors using a Polytron homogenizer. Tissue lysates containing measured amount of proteins (33) were analyzed by SDS/PAGE under reducing conditions and subjected to Western blotting. Production of antihuman and antimouse CAIV were described earlier (2, 6) and were used at 1:3,000 dilutions. Antitubulin (Sigma-Aldrich) was used at 1:6,000 dilution. Anti-rabbit IgG-peroxidase (Sigma-Aldrich) was used as secondary antibody at 1:4,000 dilution. Bands were detected by chemiluminescence detection method.

Tissue Histology. Kidneys dissected after formalin perfusion were fixed, dehydrated, paraffin-embedded, and sectioned according to standard procedures. Histological sections were stained with H&E and examined under a light microscope.

TUNEL Staining and Immunofluorescence. Apoptotic cells in kidney sections were detected using TUNEL assay kit (Roche Applied Science) according the manufacturer's protocol. Apoptotic cells were quantified by counting the number of TUNEL-positive cells in at least five fields from several age-, sex-, and genotype-matched mice and the values were expressed as a percentage of total number of cells in the field as determined by DAPI staining. Statistical significance of difference between groups was evaluated by an unpaired Student *t* test with GraphPad Prism software, where P values <0.05 were considered statistically significant. Immunofluorescence on kidney sections was done by standard method of deparaffinization and rehydration of the tissues followed by procedures as described previously for immunofluorescence-based detection of BiP in cell culture (34).

RNA Isolation, RT-PCR, and RT-qPCR. Total RNA from kidney was prepared by using an RNAeasy kit (Qiagen). RT-PCR and RT-qPCR were performed according to the procedure described earlier (2, 10). The following primers were used: human CAIV (forward), 5′-TTGCTGTCCCGCAAGATGCGGATG-3′; human CAIV (reverse), 5′-AGAAATGCTGGCCTTGTTCTCCAGC-3′; mouse BiP (forward), 5′-CCTGCGTCGGTGTGTTCAAG-3′; mouse BiP (reverse), 5′-AAGGGTCATTCCAAGTGCG-3′; mouse β-actin (forward), 5′-AGCCATGTACGTAGCCATCCAGGCTGTG-3′; mouse β-actin (reverse), 5′-TGGGTACATGGTGGTACCACCAGACAGC-3′. All reactions were carried out in duplicate with RNAs from at least three animals in each group. The relative transcript level of the target gene was calculated as previously described (34). Statistical significance of difference between groups was evaluated by an unpaired Student *t* test using the GraphPad Prism software, where P values <0.05 were considered statistically significant.

ACKNOWLEDGMENTS. The authors would like to thank Dr. Jan Ryerse for the use of his microscope facility, Dr. Yun Tan for technical assistance during the early part of this work, and Tracey Baird for editorial assistance in the preparation of this manuscript. This work was supported by National Institutes of Health Grants GM34182 and DK040163 (to W.S.S.) and AI022646 (to M.G.K.).

1. Zhu XL, Sly WS (1990) Carbonic anhydrase IV from human lung. Purification, characterization, and comparison with membrane carbonic anhydrase from human kidney. *J Biol Chem* 265:8795–8801.
2. Shah GN, et al. (2005) Carbonic anhydrase IV and XIV knockout mice: roles of the respective carbonic anhydrases in buffering the extracellular space in brain. *Proc Natl Acad Sci USA* 102:16771–16776.
3. Brown D, Zhu XL, Sly WS (1990) Localization of membrane-associated carbonic anhydrase type IV in kidney epithelial cells. *Proc Natl Acad Sci USA* 87:7457–7461.
4. Ogilvie JM, et al. (2007) Carbonic anhydrase XIV deficiency produces a functional defect in the retinal light response. *Proc Natl Acad Sci USA* 104:8514–8519.
5. Innocenti A, et al. (2005) Carbonic anhydrase inhibitors. Inhibition of the membrane-bound human and bovine isozymes IV with sulfonamides. *Bioorg Med Chem Lett* 15: 1149–1154.
6. Rebello G, et al. (2004) Apoptosis-inducing signal sequence mutation in carbonic anhydrase IV identified in patients with the RP17 form of retinitis pigmentosa. *Proc Natl Acad Sci USA* 101:6617–6622.
7. Yang Z, et al. (2005) Mutant carbonic anhydrase 4 impairs pH regulation and causes retinal photoreceptor degeneration. *Hum Mol Genet* 14:255–265.
8. Alvarez BV, et al. (2007) Identification and characterization of a novel mutation in the carbonic anhydrase IV gene that causes retinitis pigmentosa. *Invest Ophthalmol Vis Sci* 48:3459–3468.
9. Bonapace G, Waheed A, Shah GN, Sly WS (2004) Chemical chaperones protect from effects of apoptosis-inducing mutation in carbonic anhydrase IV identified in retinitis pigmentosa 17. *Proc Natl Acad Sci USA* 101:12300–12305.
10. Datta R, Waheed A, Bonapace G, Shah GN, Sly WS (2009) Pathogenesis of retinitis pigmentosa associated with apoptosis-inducing mutations in carbonic anhydrase IV. *Proc Natl Acad Sci USA* 106:3437–3442.
11. Wu J, Kaufman RJ (2006) From acute ER stress to physiological roles of the unfolded protein response. *Cell Death Differ* 13:374–384.
12. Rutkowski DT, Kaufman RJ (2004) A trip to the ER: coping with stress. *Trends Cell Biol* 14:20–28.
13. Schwartz GJ (2002) Physiology and molecular biology of renal carbonic anhydrase. *J Nephrol* 15 (Suppl 5):S61–S74.
14. Ladiges WC, et al. (2005) Pancreatic beta-cell failure and diabetes in mice with a deletion mutation of the endoplasmic reticulum molecular chaperone gene P58IPK. *Diabetes* 54:1074–1081.
15. Rutkowski DT, et al. (2007) The role of p58IPK in protecting the stressed endoplasmic reticulum. *Mol Biol Cell* 18:3681–3691.
16. Oyadomari S, et al. (2002) Targeted disruption of the Chop gene delays endoplasmic reticulum stress-mediated diabetes. *J Clin Invest* 109:525–532.
17. Socha L, Silva D, Lesage S, Goodnow C, Petrovsky N (2003) The role of endoplasmic reticulum stress in nonimmune diabetes: NOD.k iHEL, a novel model of beta cell death. *Ann N Y Acad Sci* 1005:178–183.
18. Park KM, Kim JI, Ahn Y, Bonventre AJ, Bonventre JV (2004) Testosterone is responsible for enhanced susceptibility of males to ischemic renal injury. *J Biol Chem* 279:52282–52292.
19. Inagi R (2009) Endoplasmic reticulum stress in the kidney as a novel mediator of kidney injury. *Nephron Exp Nephrol* 112:e1–e9.
20. Kitamura M (2008) Endoplasmic reticulum stress and unfolded protein response in renal pathophysiology: Janus faces. *Am J Physiol Renal Physiol* 295:F323–F334.
21. Bando Y, et al. (2004) ORP150/HSP12A protects renal tubular epithelium from ischemia-induced cell death. *FASEB J* 18:1401–1403.
22. Lindenmeyer MT, et al. (2008) Proteinuria and hyperglycemia induce endoplasmic reticulum stress. *J Am Soc Nephrol* 19:2225–2236.
23. Liu F, Inageda K, Nishitai G, Matsuoka M (2006) Cadmium induces the expression of Grp78, an endoplasmic reticulum molecular chaperone, in LLC-PK1 renal epithelial cells. *Environ Health Perspect* 114:859–864.
24. Ohse T, et al. (2006) Albumin induces endoplasmic reticulum stress and apoptosis in renal proximal tubular cells. *Kidney Int* 70:1447–1455.
25. Liu L, et al. (2001) Defective nephrin trafficking caused by missense mutations in the NPHS1 gene: insight into the mechanisms of congenital nephrotic syndrome. *Hum Mol Genet* 10:2637–2644.
26. Zivná M, et al. (2009) Dominant renin gene mutations associated with early-onset hyperuricemia, anemia, and chronic kidney failure. *Am J Hum Genet* 85:204–213.
27. Cohen E, Bieschke J, Perciavalle RM, Kelly JW, Dillin A (2006) Opposing activities protect against age-onset proteotoxicity. *Science* 313:1604–1610.
28. Morley JF, Brignull HR, Weyers JJ, Morimoto RI (2002) The threshold for polyglutamine-expansion protein aggregation and cellular toxicity is dynamic and influenced by aging in Caenorhabditis elegans. *Proc Natl Acad Sci USA* 99:10417–10422.
29. Naidoo N (2009) The endoplasmic reticulum stress response and aging. *Rev Neurosci* 20:23–37.
30. Ben-Zvi A, Miller EA, Morimoto RI (2009) Collapse of proteostasis represents an early molecular event in Caenorhabditis elegans aging. *Proc Natl Acad Sci USA* 106: 14914–14919.
31. Oyadomari S, et al. (2006) Cotranslocational degradation protects the stressed endoplasmic reticulum from protein overload. *Cell* 126:727–739.
32. Okuyama T, Batanian JR, Sly WS (1993) Genomic organization and localization of gene for human carbonic anhydrase IV to chromosome 17q. *Genomics* 16:678–684.
33. Peterson GL (1979) Review of the Folin phenol protein quantitation method of Lowry, Rosebrough, Farr and Randall. *Anal Biochem* 100:201–220.
34. Datta R, Waheed A, Shah GN, Sly WS (2007) Signal sequence mutation in autosomal dominant form of hypoparathyroidism induces apoptosis that is corrected by a chemical chaperone. *Proc Natl Acad Sci USA* 104:19989–19994.